# NACA

# RESEARCH MEMORANDUM

EXPERIMENTAL INVESTIGATION OF A FIVE-STAGE AXIAL-FLOW

RESEARCH COMPRESSOR WITH TRANSONIC ROTORS

IN ALL STAGES

II - COMPRESSOR OVER-ALL PERFORMANCE

By Karl Kovach and Donald M. Sandercock

Lewis Flight Propulsion Laboratory
Cleveland, Ohio

# NATIONAL ADVISORY COMMITTEE
# FOR AERONAUTICS

WASHINGTON

J

NATIONAL ADVISORY COMMITTEE FOR AERONAUTICS

RESEARCH MEMORANDUM

EXPERIMENTAL INVESTIGATION OF A FIVE-STAGE AXIAL-FLOW RESEARCH

COMPRESSOR WITH TRANSONIC ROTORS IN ALL STAGES

II - COMPRESSOR OVER-ALL PERFORMANCE

By Karl Kovach and Donald M. Sandercock

## SUMMARY

As the initial step in an investigation of the potential performance and problems associated with a high-stage-pressure-ratio compressor in which all rotor stages operate at transonic tip relative inlet Mach numbers, the over-all performance of a 20-inch-diameter five-stage compressor was evaluated. The compressor, which was installed as a component of an existing turbojet engine, was designed to produce a pressure ratio of 5.0 (average stage total-pressure ratio of 1.38) and an equivalent weight flow of 67.5 pounds per second [31 (lb/sec)/sq ft rotor frontal area] at an adiabatic efficiency of 0.85. The design equivalent tip speed was 1100 feet per second.

The over-all performance was evaluated over a range of flows at equivalent tip speeds from 40 to 100 percent of design. The maximum total-pressure ratio obtained at design speed was 5.0 at an equivalent weight flow of 69.8 pounds per second with an adiabatic efficiency of 0.81. Good efficiency characteristics were obtained over the speed range investigated. The peak efficiency for a given compressor speed increased from 0.77 at 40 percent of design to a maximum of 0.87 at approximately 85 percent of design speed and decreased to 0.81 at design speed.

## INTRODUCTION

In order to investigate the possibilities of and to evaluate the problems associated with a high-mass-flow, high-stage-pressure-ratio compressor in which all rotor stages operate at transonic tip relative inlet Mach numbers, a five-stage 20-inch-diameter compressor was designed and constructed at the NACA Lewis laboratory. The design average stage pressure ratio was 1.38 and the design specific mass flow was 31 pounds per second per square foot of rotor frontal area. The design details for this compressor are discussed in reference 1.

The over-all compressor performance will be presented and discussed in this report on the basis of total-pressure ratio, adiabatic efficiency, inlet and discharge flow variations, and blade-row and stage static-pressure-ratio distribution through the compressor.

## SYMBOLS

The following symbols are used in this report:

$A_f$     rotor frontal area, sq ft

$M'$     Mach number relative to blade row

$P$     absolute total pressure, lb/sq ft

$T$     absolute total temperature, $^\circ$R

$W$     air weight flow, lb/sec

$\beta'$     air-flow angle relative to blade measured from axial direction, deg

$\gamma^\circ$     blade angle, angle between tangent to blade mean line at leading or trailing edge and axial direction, deg

$\delta$     ratio of inlet total pressure to NACA standard sea-level pressure, $P_1/2116.2$

$\eta$     adiabatic temperature-rise efficiency

$\theta$     ratio of inlet total temperature to NACA standard sea-level temperature, $T_1/518.6$

Subscripts:     (see fig. 3)

0     bellmouth inlet

1     compressor flow-measuring station

2,4,6,8,10     stations ahead of rotors 1, 2, 3, 4, and 5, respectively

3,5,7,9,11     stations ahead of stators 1, 2, 3, 4, and 5, respectively

12     station at fifth-stator discharge

13     compressor-discharge measuring station

## APPARATUS AND INSTRUMENTATION

### Compressor Design Specifications

A complete description of the aerodynamic designs and the geometry of the five-stage transonic compressor is presented in reference 1. Some of the pertinent design values are summarized as follows:

Total-pressure ratio . . . . . . . . . . . . . . . . . . . . . . 5.0
Average stage pressure ratio . . . . . . . . . . . . . . . . . . 1.38
Over-all efficiency . . . . . . . . . . . . . . . . . . . . . . 0.85
Inlet hub-tip radius ratio . . . . . . . . . . . . . . . . . . . 0.50
Equivalent weight flow, lb/sec . . . . . . . . . . . . . . . . . 67.5
Equivalent weight flow, (lb/sec)/sq ft rotor frontal area . . . 31
Equivalent tip speed, ft/sec . . . . . . . . . . . . . . . . . . 1100

### Engine Installation

The over-all performance results reported herein were obtained when the compressor was operated as a component of an existing turbojet engine in order to obtain a convenient power source. Figure 1 is a photograph of the compressor, with the top casing removed, installed in the engine. The engine was a commercial unit in the 3000-pound-thrust class, consisting of a double annular combustion chamber and a two-stage turbine. All parts used in this installation, except the compressor rotor, casings, and diffuser, were standard engine parts.

The engine was equipped with an inlet bellmouth that conformed to A.S.M.E. flow-nozzle specifications to meter the air and ensure smooth flow at the compressor inlet. In order to vary the compressor air flow, the engine was equipped with a variable-area exhaust nozzle. To meet the compressor power requirements and obtain additional flow-range control, the flow area of the first-stage turbine stators was varied. The stators were not adjustable during operation, but the flow-area range was obtained by constructing several sets of turbine stators with different area settings and replacing them as required. When the engine was equipped with the turbine stators having the smallest flow area, it could not be accelerated. Compressor surge was encountered at low engine speeds, and the use of compressor bleed was required for acceleration. Air was bled from the engine diffuser about 10 inches downstream of the compressor discharge through eight tubes spaced circumferentially on the diffuser outer wall. The tubes discharged into a common collector. The air was discharged from the collector through a single large pipe. The compressor-bleed system was manually controlled by means of a valve in the collector discharge pipe. Figure 2 is a photograph of the engine installation.

## Instrumentation

Pressures were measured with manometers containing mercury and tetrabromoethane, and temperatures were measured with a self-balancing potentiometer. The compressor speed was measured with a chronometric tachometer.

Engine bellmouth inlet. - The instrumentation at the engine bellmouth inlet (station 0, fig. 3) consisted of a cross rake (fig. 2) containing ten bare-wire thermocouples and three total-pressure tubes. These readings were considered to be the compressor-inlet stagnation conditions.

Compressor flow-measuring station. - The compressor flow-measuring station (station 1, fig. 3) was approximately $10\frac{1}{2}$ inches upstream of the rotor in the constant-area portion of the inlet bellmouth. At this station was located a five-tube radial static-pressure rake (fig. 4(a)) with the tubes equally spaced across the passage. In the same axial plane, on the outer wall of the bellmouth, were six static-pressure orifices equally spaced around the circumference. Also in the same axial plane were two five-tube boundary-layer rakes (fig. 4(b)), one at the outer wall and one at the inner wall. The rakes were $180^{\circ}$ apart and each rake covered about 0.6 inch of the total passage height. The sketch shown in figure 5(a) indicates the relative circumferential locations of the instruments at this station.

Compressor inlet. - At the compressor inlet (station 2, fig. 3) four equally spaced static-pressure orifices were located on both the inner and outer walls. Because the rotor blades have a radial taper when projected to the axial plane, the outer- and inner-wall orifices were 0.75 and 0.40 inch upstream of the first-rotor leading edge, respectively.

Blade-row outlet. - At the outlet of each blade row (stations 3 to 12, fig. 3), four static-pressure orifices were located on the outer wall. The orifices were equally spaced circumferentially approximately 0.9 inch behind the rotor blade trailing edge and approximately 0.3 inch behind the stator blade trailing edge.

Compressor discharge. - The compressor-discharge station was approximately 2 inches downstream of the fifth-stator trailing edge (station 13, fig. 3). The instrumentation at this station consisted of four fixed Kiel-type total-pressure rakes (fig. 4(c)) with five equally spaced pressure tubes per rake, and four fixed bare-wire spike-type thermocouple rakes (fig. 4(d)) with five equally spaced thermocouples per rake. Both types of rake were located at centers of four equally spaced circumferential portions of one complete blade passage. This station also had four equally spaced static-pressure orifices on both the inner and outer walls. Three self-balancing and actuator-operated claw - total-pressure probes (fig. 4(e)) indicated that no correction to the total-temperature and total-pressure readings for the effects of flow angle were necessary.

The temperature readings were corrected for local Mach number effects. The relative circumferential locations of the instruments at this station are shown by the sketch in figure 5(b).

Accuracy. - The accuracy of the measurements is estimated to be within the following limits:

Temperature, °F . . . . . . . . . . . . . . . . . . . . . . . . .   ±1.0
Pressure, in. Hg . . . . . . . . . . . . : . . . . . . . . . . .   ±0.05
Weight flow, percent . . . . . . . . . . . . . . . . . . . . . .   ±1.0
Speed, percent . . . . . . . . . . . . . . . . . . . . . . . . .   ±0.5

## PROCEDURE

### Operation

All tests were conducted by drawing air directly from the atmosphere, with the result that no control of the compressor-inlet conditions could be employed. The compressor was operated at constant equivalent tip speeds of 40, 50, 70, 80, 90, 95, and 100 percent of design speed. The range of air flows investigated extended from maximum flow (maximum-area first-stage turbine stator and wide-open exhaust nozzle) to a flow where surge was encountered or to a flow where operation was limited by the turbine-inlet temperature. This range of compressor air flows was not completely investigated at equivalent speeds of 40 and 50 percent of design, because increased compressor blade vibrations were observed in the speed range from 40 to 70 percent of design and further extended operation in this speed range was deferred.

### Calculations

Compressor air flow. - The air flow through the compressor was calculated from the measurements (at station 1) of the radial variation of static pressure given by the static-pressure rake and the wall orifices, the inlet stagnation conditions, and a wall boundary-layer blockage allowance determined from the measurements of total pressure from the boundary-layer rakes. A discussion of the boundary-layer blockage allowance and its determination is given in reference 1. For these tests, the boundary-layer blockage factor was found to be constant at a value of 0.981 for the entire air-flow range. References 2 and 3 indicate the reliability of this air-flow measuring method.

Compressor inlet. - All computations of compressor-inlet air angles and velocities (station 2) were based on considering the absolute inlet velocity to be axial in direction (no inlet guide vanes). A linear variation of static pressure was assumed to exist between the averages of the outer- and inner-wall measurements. In the design (ref. 1), because of

the approximate symmetry of the casing fairings at the first-rotor in-
let, the flow was considered to be uniform across the radial height of
the annulus.  The compressor-inlet stagnation conditions were considered
to be the same as the conditions measured at the engine bellmouth inlet
(station 0).

Compressor discharge. - At each flow point, the discharge total
pressure was obtained by two methods.  The measured discharge total pres-
sure was the arithmetic average of the four five-tube fixed-pressure-rake
measurements.  The calculated discharge total pressure was obtained by
the method presented in reference 4.  In this method, the measured values
of discharge static pressure, total temperature, weight flow, and area
normal to the compressor axis are used to determine the discharge total
pressure from the energy and continuity equations.  The assumptions of
this method do not credit the compressor for nonuniformity of veloci-
ty and deviation from axial discharge, and therefore the calculated val-
ues will usually be lower than the measured values.  For the test results
presented herein, large velocity gradients were not encountered, and pres-
sures determined by the two methods were approximately equal.  The adia-
batic temperature-rise efficiency was calculated by using the calculated
discharge total-pressure ratio to determine the isentropic power input
and the arithmetic average of the four five-spike thermocouple-rake read-
ings to determine the actual power input.  The over-all performance char-
acteristics of the compressor are presented in terms of the pressure
ratios as determined from the calculated discharge total pressure.

To determine the radial variation of total pressure, total tempera-
ture, and adiabatic efficiency of the compressor discharge (station 13),
the arithmetic average of the four pressure and temperature readings at
each of the five radial stations was used.  In the determination of the
radial variation of discharge velocity, a linear variation of static
pressure was assumed to exist between the outer- and inner-wall
measurements.


RESULTS AND DISCUSSION

Over-All Performance

The over-all total-pressure characteristics of the compressor are
presented in figure 6 as the conventional plot of total-pressure ratio
against equivalent weight flow over a range of equivalent speeds from 40
to 100 percent of design.  The maximum pressure ratio obtained at design
speed was 5.00 (average stage total-pressure ratio = 1.38) and occurred
at an equivalent weight flow of 69.8 pounds per second [32 (lb/sec)/sq ft
frontal area].  This peak operating point was not a surge point for the
compressor.  Operation beyond this point was not attempted because of

the limiting turbine temperature.  In fact, in the performance map of
figure 6 audible compressor surge was encountered only at speeds of 50,
70, and 80 percent of design.

The efficiency characteristics of the compressor are shown in the
upper part of figure 6, with the adiabatic temperature-rise efficiency
plotted as a function of equivalent weight flow for a range of equiva-
lent speeds from 40 to 100 percent of design.  The maximum peak effi-
ciency of 0.87 is obtained between 80 and 90 percent of design speed
range.  Good efficiency characteristics are obtained over the entire
speed range, as is indicated by the peak-efficiency line of this figure.
The peak efficiency for a given compressor speed increases from 0.77 at
40 percent of design speed to the maximum value of 0.87 and then de-
creases to 0.81 at design speed.

## Compressor-Inlet Conditions

The radial variation of relative inlet Mach number and relative
inlet-air angle for the first rotor (station 2, fig. 3) is shown in
figure 7 at the peak over-all efficiency point for equivalent speeds of
80, 90, 95, and 100 percent of design.  At design speed, because the
weight flow exceeded the design value, the relative inlet Mach number
was higher than the design value and the relative inlet-air angles and
incidence angles were lower than the design values, as indicated in fig-
ure 7.  (Incidence angle, which is defined as the angle between the
relative inlet-air velocity vector and a tangent to the blade mean line
at the leading edge, is the difference between the relative air angle
and blade mean-line angle in fig. 7).  A maximum inlet Mach number of
1.24 was obtained at the blade tip of the first rotor, and approximately
60 percent of the blade span was operating at relative Mach numbers
greater than 1.  Figure 7 also indicates that, from 80 to 100 percent of
design speed, the compressor was operating at transonic tip relative
inlet Mach numbers.

## Compressor-Discharge Conditions

Comparison of the radial variation of total temperature, total-
pressure ratio, adiabatic efficiency, and velocity at the compressor
discharge (station 13, fig. 3) with design variations is shown in fig-
ure 8 for the peak-efficiency points at equivalent tip speeds of 90, 95,
and 100 percent of design.  Although the compressor was designed for
radially constant work input (ref. 1), a radial work-input gradient was
measured as indicated by the temperature variation (fig. 8).  The total
pressure was, however, essentially constant over the portion of the pas-
sage covered by the instrumentation.  The adiabatic efficiency was com-
puted from the measured variations of total temperature and total

pressure. Although no radial measurements of static pressure were made, the orifices at the outer and inner walls indicated only a slight static-pressure gradient. At design speed the average discharge velocity of approximately 495 feet per second is somewhat less than the design average discharge velocity of 520 feet per second.

## Stagewise Variation of Static Pressure

The static-pressure distribution through the compressor as measured at the tip for the peak-pressure-ratio point at design speed is compared with the design values in figure 9. This figure shows the static-pressure ratio across each blade row, the static-pressure ratio across each stage, and the ratio of the static pressure at each station to the inlet total pressure. Good agreement was obtained between the measured and design values.

## Performance Evaluation

For operation of the compressor at the design equivalent tip speed, figure 6 indicates that, although design total-pressure ratio was attained, the maximum equivalent weight flow obtained exceeded the design value of 67.5 pounds per second, and the peak efficiency was lower than both the maximum peak efficiency of 0.87 and the design assumption of 0.85. Evaluation of stage performance on the basis of static-pressure ratio (fig. 9) indicates that each stage is operating near its design value of static-pressure ratio, with a trend towards slightly higher than design static-pressure ratio in the latter stages.

The effects of the increased flow through the compressor on the conditions at the inlet to the first rotor were pointed out in the discussion of figure 7. It was observed that the relative inlet Mach number was considerably higher than the design value and that the incidence angle was considerably lower than design and varied slightly radially (approx. $0°$ at hub and $1°$ at tip) in contrast to the radially constant design positive value of $4°$. The design value of incidence angle was chosen from the performance results of reference 5 plus an anticipated increase in incidence angle for the higher Mach number level. On the basis of the data of reference 5, the first rotor was apparently not operating at its minimum-loss incidence angle. This reference indicates the sharp rise in loss (therefore drop in efficiency) at rotor incidence angles below the minimum-loss angle at high inlet Mach numbers. This effect would be especially detrimental to the performance in the tip region. The observations of low incidence angle for the first rotor with probable low tip efficiency and apparently insufficient turning are inconsistent with the close agreement between the measured and design static-pressure ratio across the first rotor (fig. 9). This agreement

could occur only if the blade were overcambered, the area allowance for boundary layer were too large, or the design rotor efficiency assumption were too low (all of these factors affecting the axial-velocity ratio and therefore the work input across the blade row). Recent considerations of the deviation-angle characteristics (ref. 6) indicate that the design deviation angles (defined as the difference between the angle of the air leaving the blade and the angle of the tangent to the mean line at the blade trailing edge) selected for the first rotor were too high, especially at the tip, and resulted in an overcambered blade section. Reference 6 also indicates the deviation-angle sensitivity of the rotor tip region in terms of pressure ratio. Therefore, even though the blade row was operating at a low incidence angle, design turning was probably obtained because the blade was overcambered. In the design, the blockage factor for the first stage was chosen from the performance results of a single-stage transonic compressor (refs. 3 and 5). It was explained in reference 1 that assumed values of stage mass-averaged efficiency instead of blade-element efficiency were used. The effects of the low design efficiency assumptions were balanced to a large extent by the operation of the first rotor in the high-loss (low-efficiency) region, especially at the tip. For the first rotor, therefore, the efficiency and boundary-layer blockage assumptions were considered to have little effect on the work input.

In reference 1, the boundary-layer blockage allowances were largely assumed for all stages except the first stage, and mass-averaged efficiencies instead of blade-element efficiencies were used. These assumptions, in addition to the probable overcambering near the rotor tip, had an effect on the axial-velocity ratio, as indicated by the lower-than-design value of discharge velocity. However, it is not possible to evaluate the contribution of each of the assumptions with the available data.

From the preceding discussion, it is believed that the compressor could not have operated at the design weight flow and design speed. Proper incidence angle at the inlet stage, in conjunction with the over-cambering of the blades, would have resulted in a pressure ratio much higher than design. This effect would be compounded in the other stages and would cause the latter stages to stall.

## SUMMARY OF RESULTS

The following results were obtained from an investigation of over-all performance of the five-stage axial-flow transonic compressor:

1. The maximum total-pressure ratio obtained at design speed was 5.00 at an equivalent weight flow of 69.8 pounds per second with an adiabatic efficiency of 0.81 compared with design values of 5.00, 67.5, and 0.85.

2. The maximum peak efficiency was 0.87 and was obtained between 80 and 90 percent of design speed.

3. Good efficiency characteristics were obtained over the entire speed range investigated. The peak efficiency increased from a value of 0.77 at 40 percent of design speed to 0.87 at approximately 85 percent of design speed and decreased to a value of 0.81 at design speed.

Lewis Flight Propulsion Laboratory
    National Advisory Committee for Aeronautics
        Cleveland, Ohio, July 6, 1954

## REFERENCES

1. Sandercock, Donald M., Kovach, Karl, and Lieblein, Seymour: Experimental Investigation of a Five-Stage Axial-Flow Research Compressor with Transonic Rotors in All Stages. I - Compressor Design. NACA RM E54F24, 1954.

2. Lieblein, Seymour, Lewis, George W., Jr., and Sandercock, Donald M.: Experimental Investigation of an Axial-Flow Compressor Inlet Stage Operating at Transonic Relative Inlet Mach Numbers. I - Over-All Performance of Stage with Transonic Rotor and Subsonic Stators up to Rotor Relative Inlet Mach Number of 1.1. NACA RM E52A24, 1952.

3. Schwenk, Francis C., Lieblein, Seymour, and Lewis, George W., Jr.: Experimental Investigation of an Axial-Flow Compressor Inlet Stage Operating at Transonic Relative Inlet Mach Numbers. III - Blade-Row Performance of Stage with Transonic Rotor and Subsonic Stator at Corrected Tip Speeds of 800 and 1000 Feet Per Second. NACA RM E53G17, 1953.

4. NACA Subcommittee on Compressors: Standard Procedures for Rating and Testing Multistage Axial-Flow Compressors. NACA TN 1138, 1946.

5. Sandercock, Donald M., Lieblein, Seymour, and Schwenk, Francis C.: Experimental Investigation of an Axial-Flow Compressor Inlet Stage Operating at Transonic Relative Inlet Mach Numbers. IV - Stage and Blade-Row Performance of Stage with Axial-Discharge Stators. NACA RM E54C26, 1954.

6. Lieblein, Seymour: Review of High-Performance Axial-Flow-Compressor Blade-Element Theory. NACA RM E53L22, 1954.
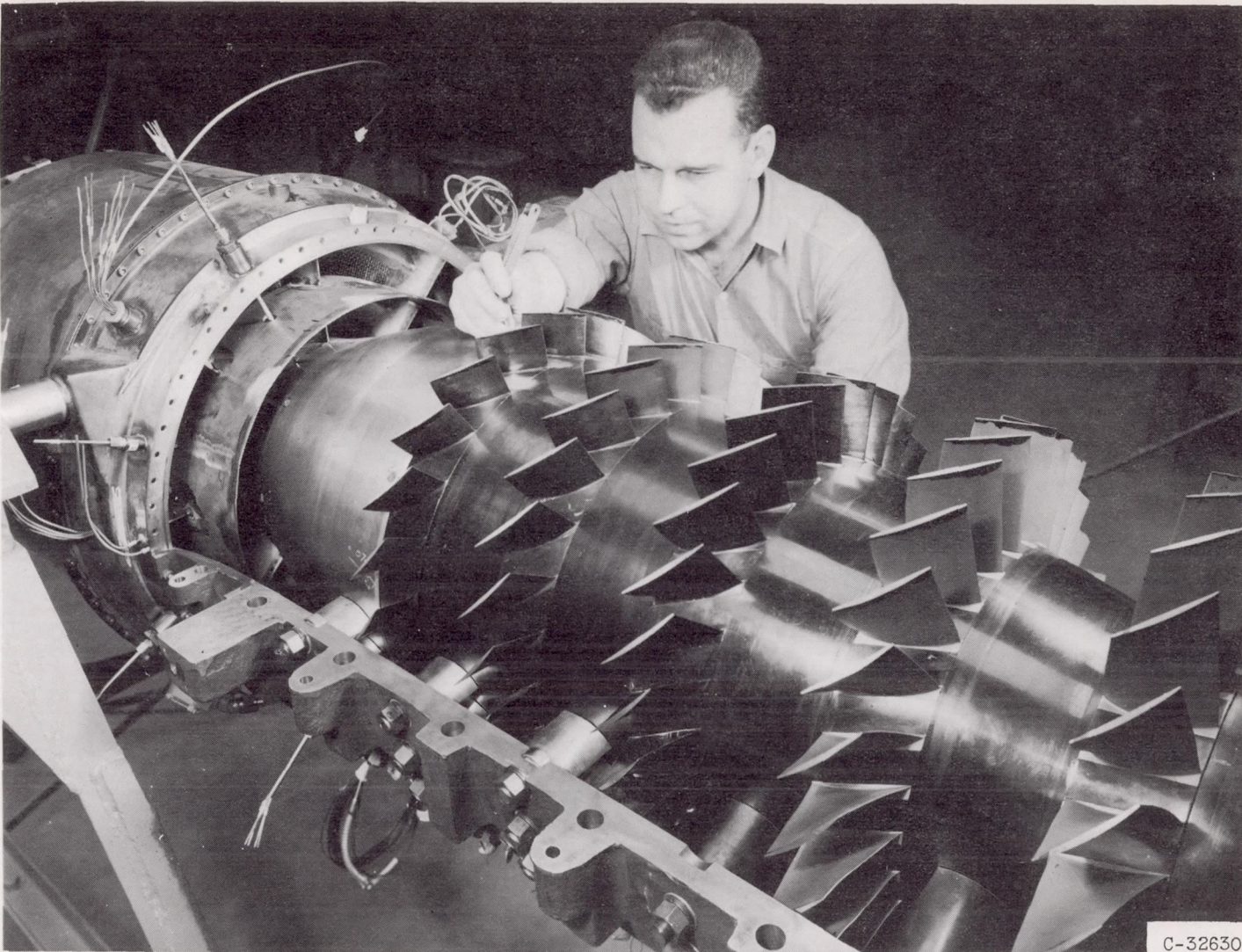
C-32630

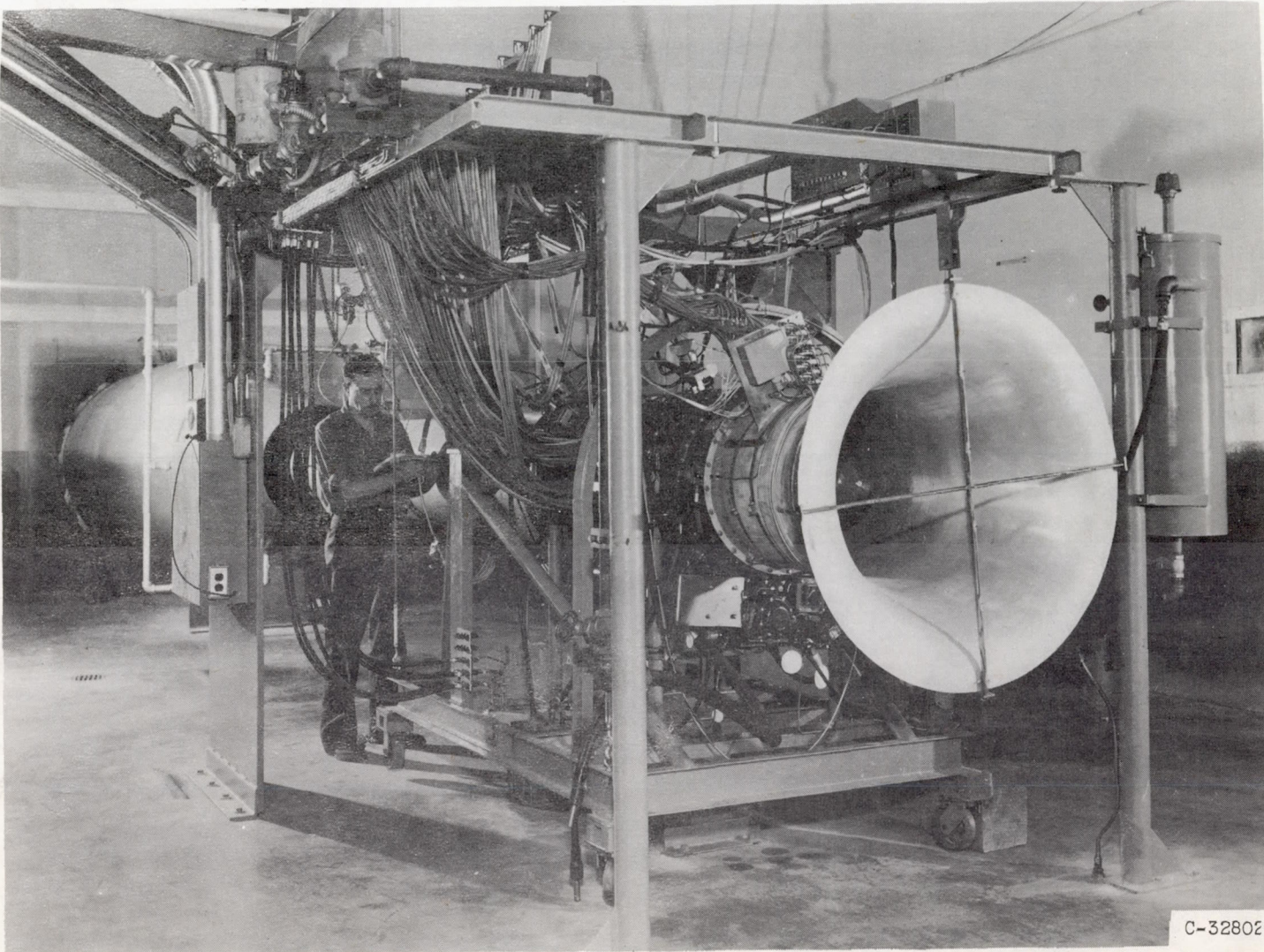Figure 1. - Five-stage axial-flow transonic compressor with upper casing removed.

Figure 2. - Test installation of five-stage axial-flow transonic compressor.
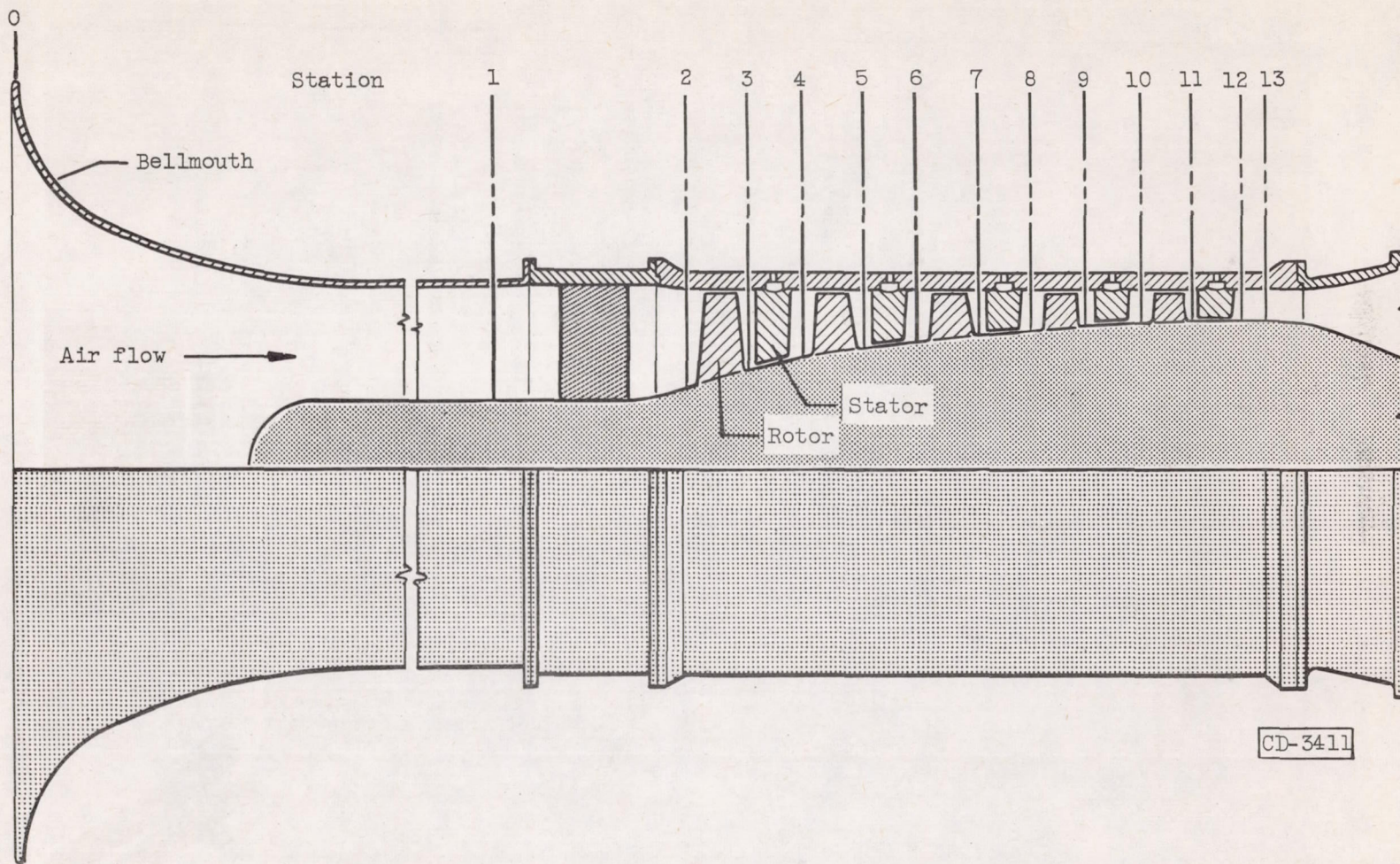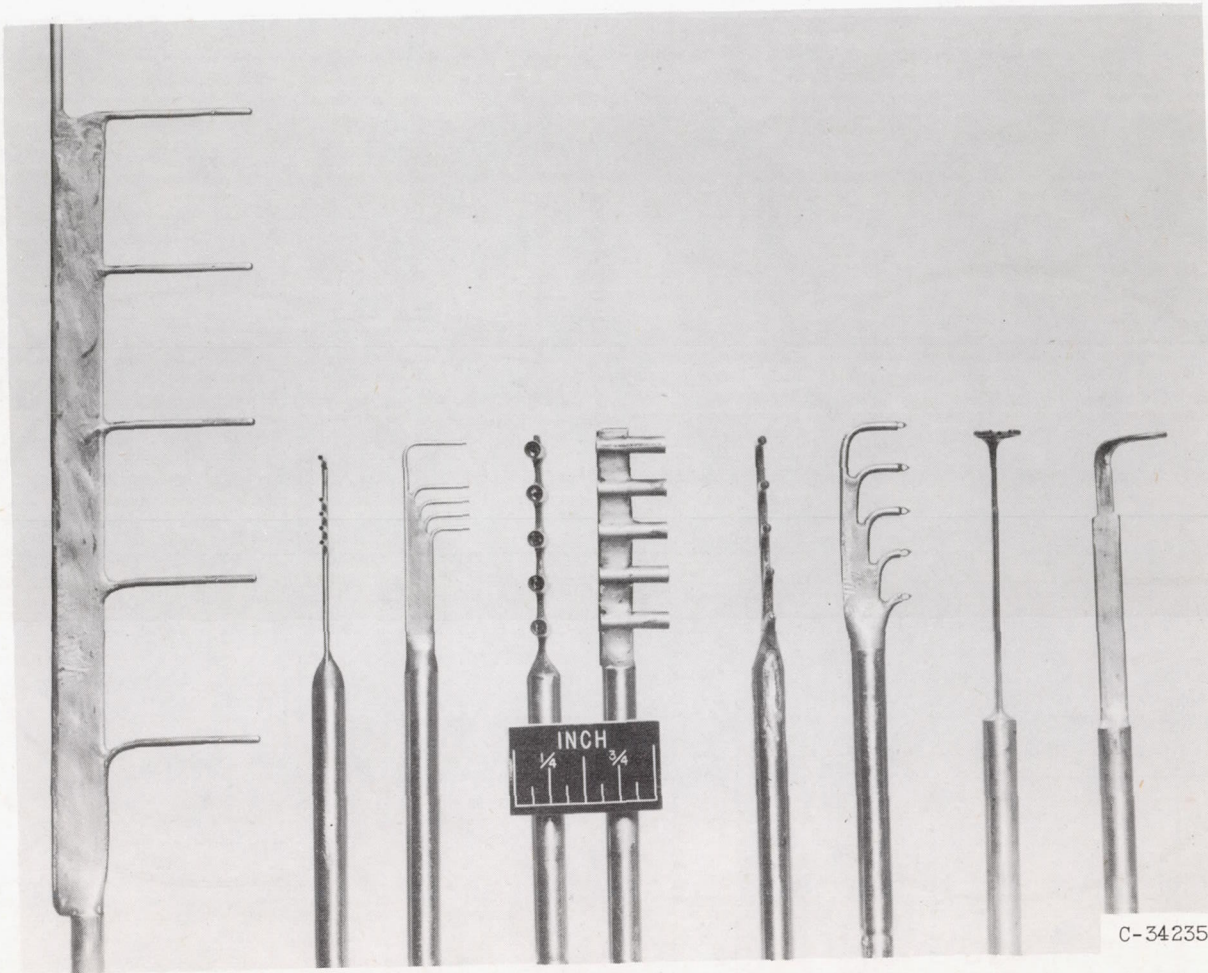
C-32802

Figure 3. - Sketch of passage contour of five-stage axial-flow transonic compressor showing axial location of blade-row inlet and outlet stations.
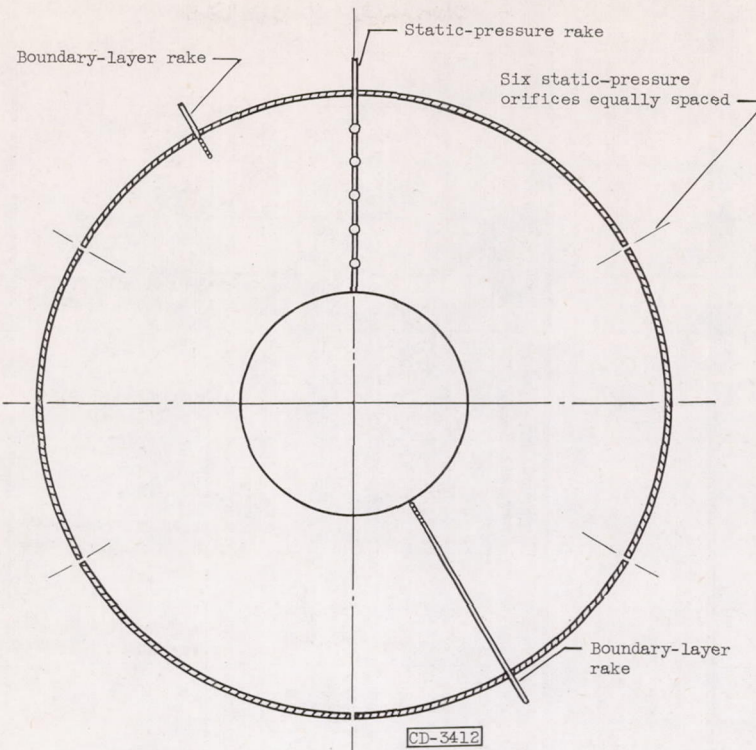
(a) Static-
pressure rake.

(b) Outer-wall
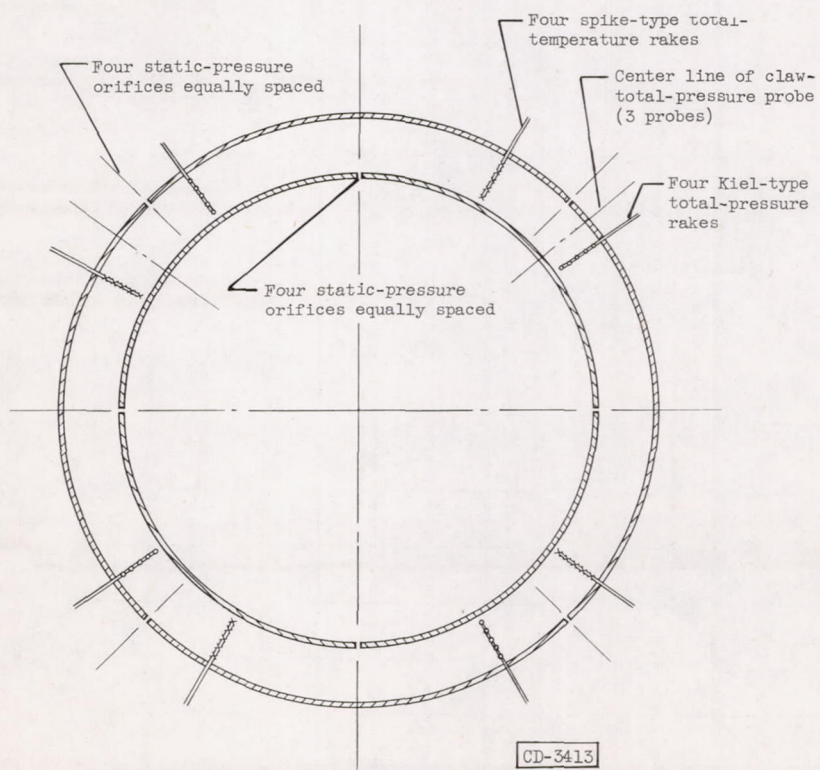boundary-
layer rake.

(c) Kiel-type
total-
pressure rake.

(d) Spike-type
total-
temperature rake.

(e) Claw - total-
pressure probe

C-34235

Figure 4. - Compressor instrumentation.

(a) Flow-measuring station (station 1).

(b) Compressor-discharge annulus (station 13).

Figure 5. - Instrumentation at two axial stations.
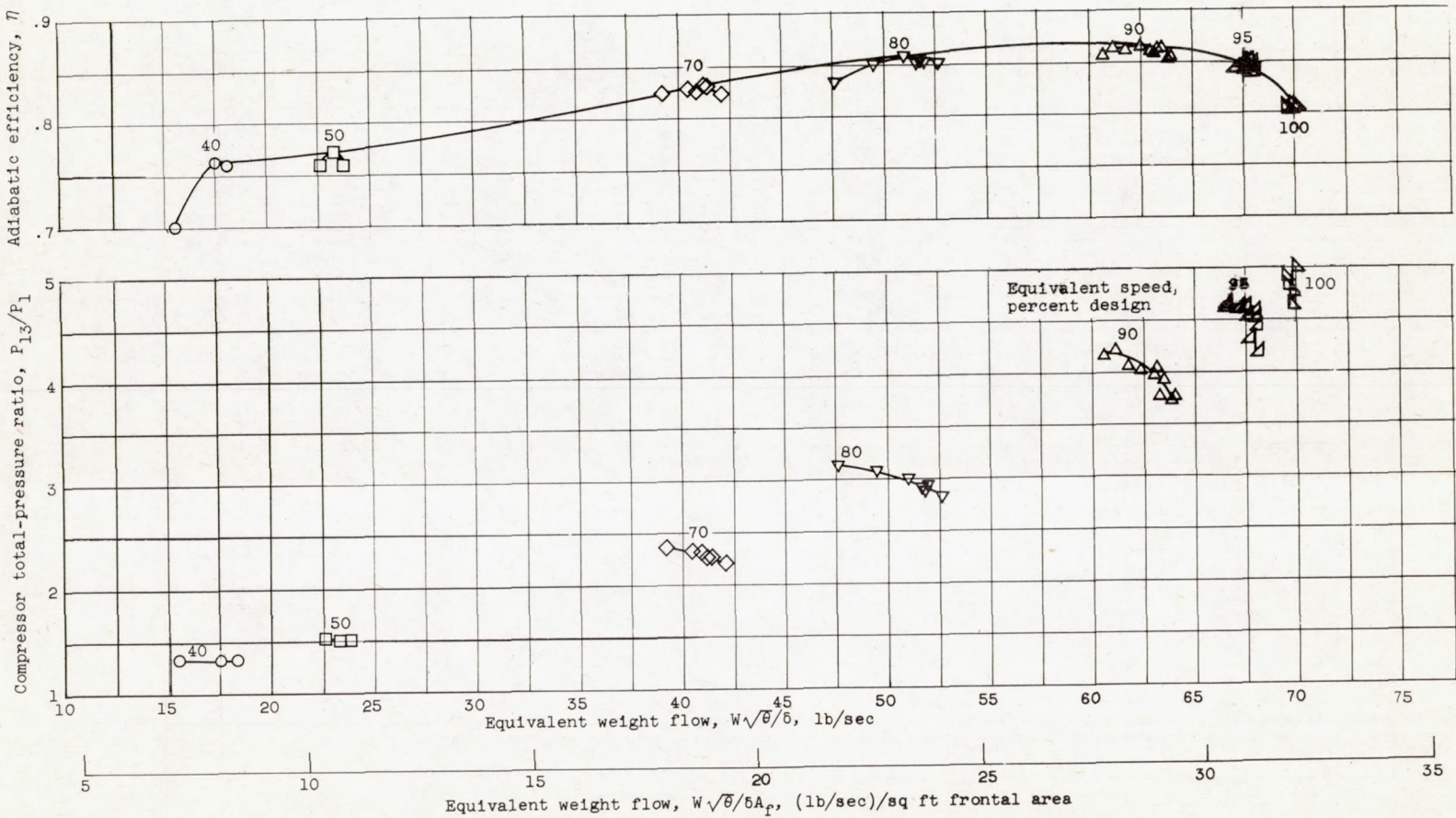
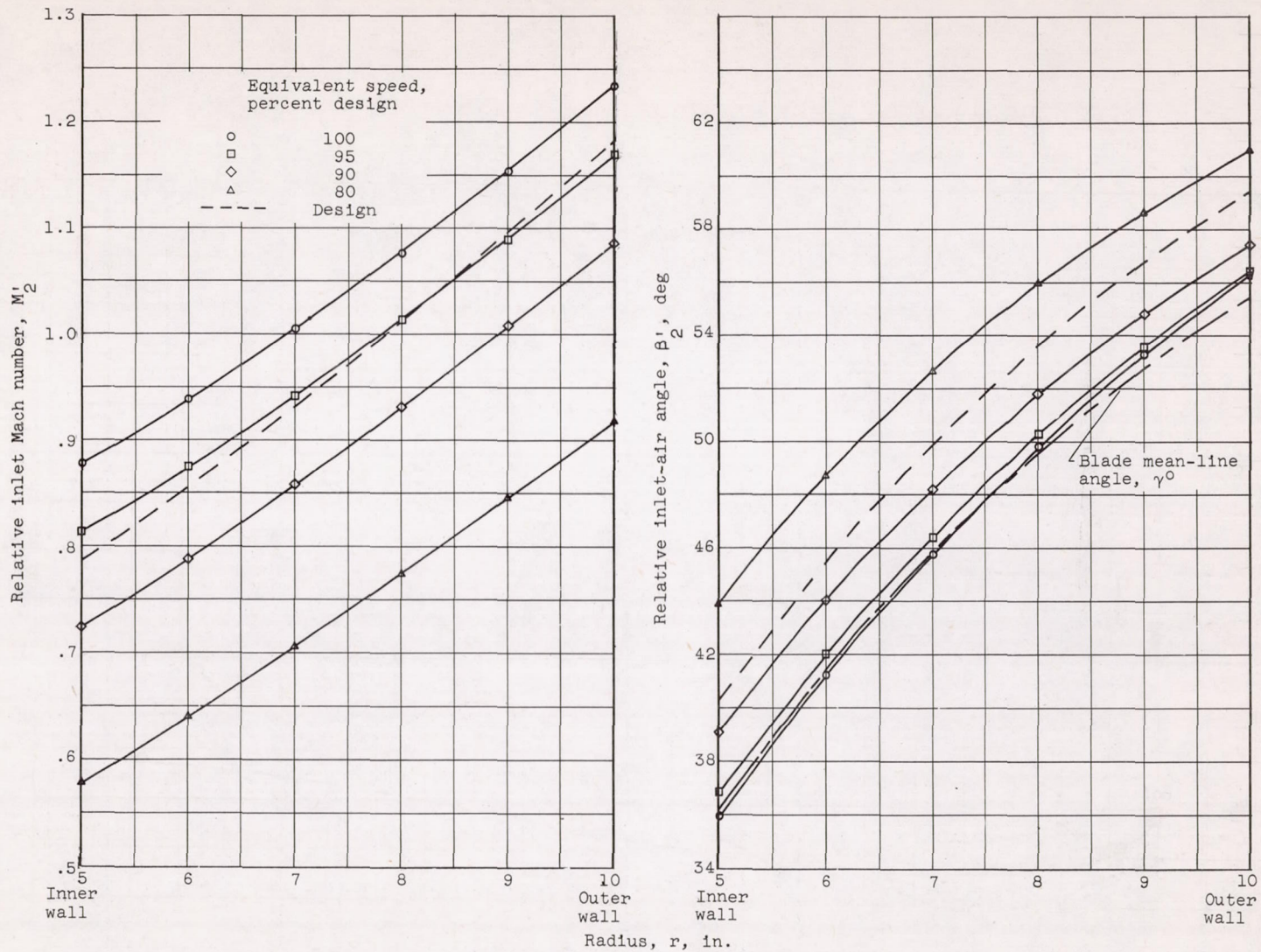Figure 6. - Over-all performance characteristics of five-stage transonic compressor.

Figure 7. - Radial variation of relative Mach number and relative air angle at compressor inlet at equivalent tip speeds of 80, 90, 95, and 100 percent of design.
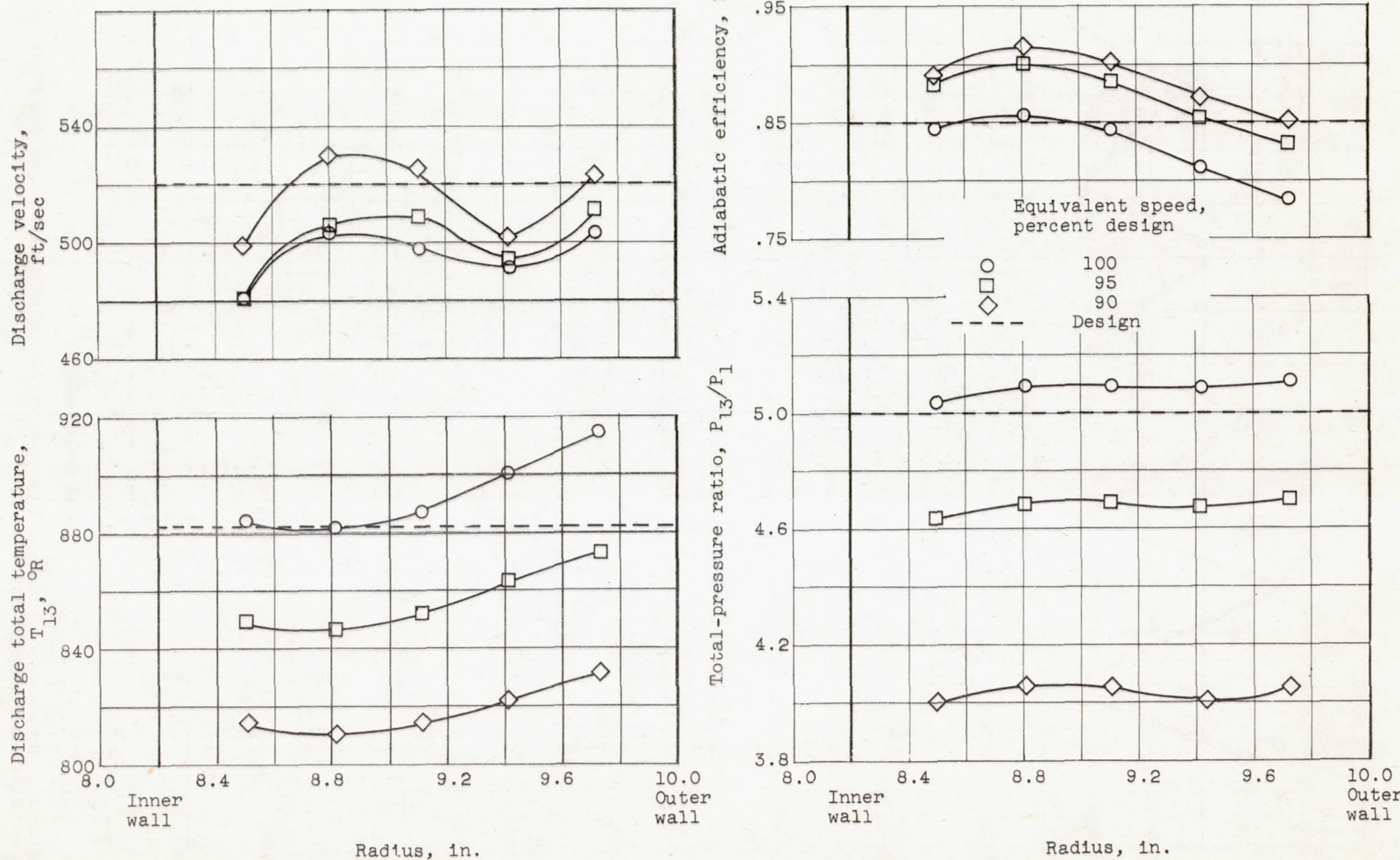
Figure 8. - Radial variation of total pressure, total temperature, adiabatic efficiency, and velocity at compressor discharge at equivalent tip speeds of 90, 95, and 100 percent of design.
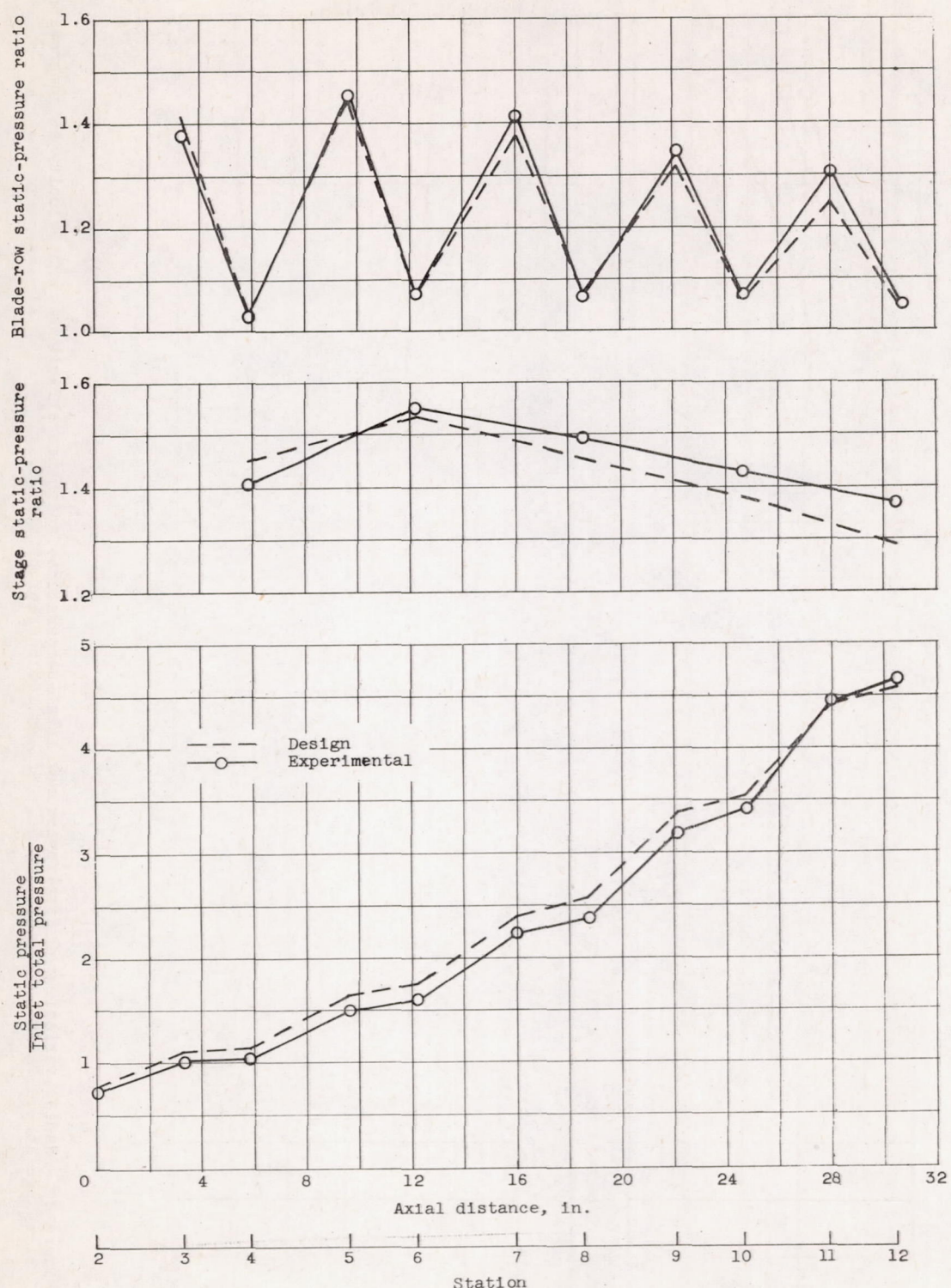
Figure 9. - Comparison of tip static-pressure ratio distribution with design at design over-all total-pressure ratio.